Pis'ma v ZhETF, vol.70, iss.7, pp.473 - 478

ANOMALOUS TEMPERATURE BEHAVIOR OF RESISTIVITY IN LIGHTLY DOPED MANGANITES AROUND A METAL-INSULATOR PHASE TRANSITION

S.Sergeenkov[+*], *M.Ausloos*[+], *H.Bougrine*[+□], *A.Rulmont*[Δ], *R. Cloots*[Δ]

[+]*SUPRAS, Institute of Physics, B5, University of Liège*
B-4000 Liège, Belgium

[*]*Bogoliubov Laboratory of Theoretical Physics, Joint Institute for Nuclear Research*
141980 Dubna, Moscow Region, Russia

[□]*SUPRAS, Montefiore Electricity Institute, B28, University of Liège,*
B-4000 Liège, Belgium

[Δ]*SUPRAS and LCIS, Institute of Chemistry,*
University of Liège, B-4000 Liège, Belgium

Submitted 10 Swptember 1999

An unusual temperature and concentration behavior of resistivity $\rho(T,x)$ in $La_{0.7}Ca_{0.3}Mn_{1-x}Cu_xO_3$ has been observed at slight Cu doping ($0 \leq x \leq 0.05$). Namely, introduction of copper results in a splitting of the resistivity maximum around a metal-insulator transition temperature $T_0(x)$ into two differently evolving peaks. Unlike the original Cu-free maximum which steadily increases with doping, the second (satellite) peak remains virtually unchanged for $x < x_c$, increases for $x \geq x_c$ and finally disappears at $x_m \simeq 2x_c$ with $x_c \simeq 0.03$. The observed phenomenon is thought to arise from competition between substitution induced strengthening of potential barriers (which hamper the charge hopping between neighboring Mn sites) and weakening of carrier's kinetic energy. The data are well fitted assuming a nonthermal tunneling conductivity theory with randomly distributed hopping sites.

PACS: 71.27.+a, 71.30.+h, 75.50.Cc

To clarify the underlying microscopic transport mechanisms in exhibiting colossal magnetoresistance manganites, numerous studies (both experimental and theoretical) have been undertaken during the past few years [1 – 17] which revealed a rather intricate correlation of structural, magnetic and charging properties in these materials based on a crucial role of the Mn^{3+}–O–Mn^{4+} network. In addition to the so-called double-exchange (DE) mechanism (allowing conducting electrons to hop from the singly occupied e_{2g} orbitals of Mn^{3+} ions to empty e_{2g} orbitals of neighboring Mn^{4+} ions), these studies emphasized the important role of the Jahn – Teller (JT) mechanism associated with the distortions of the network's bond angle and length and leading to polaron formation and electron localization in the paramagnetic insulating region. In turn, the onset of ferromagnetism below Curie point increases the effective bandwidth with simultaneous dissolving of spin polarons into band electrons and rendering material more metallic. To modify this network, the substitution effects on the properties of the most popular $La_{0.7}Ca_{0.3}MnO_3$ manganites have been studied including the isotopic substitution of oxygen ("giant" isotope effect [8, 9]), rare-earth (RE) [10 – 14] and transition element (TE) [15 – 17] doping at the Mn site. In particular, an unusually sharp *decrease* of resistivity $\rho(T)$ in $La_{0.7}Ca_{0.3}Mn_{0.96}Cu_{0.04}O_3$ due to just 4% Cu doping has been reported [17] and attributed to the Cu induced weakening of the kinetic carrier's energy $E_0(x)$. On

the other hand, the opposite temperature behavior of resistivity (that is an *increase* of ρ upon TE doping) can also be expected based on the deactivation of the DE Zener mechanism. Indeed, this mechanism is effective when electrons can hop (tunnel) between nearest-neighbor TE ions without altering their spin or energy. Hence, the observed [16] lowering of the metal-insulator (M-I) transition temperature and hopping based conductivity by TE substitution can be ascribed to an inequivalence of the ground-state energies of neighboring Mn and TE ions resulting in an appearance of the doping dependent potential barrier $U(x)$. More precisely, this potential energy exceeds the polaron bandwidth (virtually weakening the DE interaction between neighboring TE and Mn ions and impeding thus the possibility of energy-conserving coherent hops) and is defined as the difference between the binding energies of an electron on a TE ion (e.g., Cu) and Mn ion, respectively.

In an attempt to pinpoint the above-mentioned potential energy controlled hopping mechanism and gain some insight into the barrier's doping profile, in this Letter we present a comparative study of resistivity measurements on Cu doped polycrystalline manganite samples from the $La_{0.7}Ca_{0.3}Mn_{1-x}Cu_xO_3$ family for $0 \leq x \leq 0.05$ for a wide temperature interval (from 20 K to 300 K). As we shall see, the data are reasonably well fitted (for all T and x) by a unique (nonthermal) tunneling expression for the resistivity assuming a random (Gaussian) distribution of hopping sites and an explicit form for the temperature and doping dependent effective potential $U_{eff}(T,x) = U(x) - E(T,x)$. Besides, the Cu doping induced competition between the barrier's height profile $U(x)$ and the previously found [17] behavior of the carrier's kinetic energy $E_0(x) \equiv E(0,x)$ results in emergence of a satellite peak in the temperature behavior of the observed resistivity on the insulating side.

The samples examined in this study were prepared by the standard solid-state reaction from stoichiometric amounts of La_2O_3, $CaCO_3$, MnO_2, and CuO powders. The necessary heat treatment was performed in air, in alumina crucibles at 1300 C for 2 days to preserve the right phase stoichiometry. Powder X-ray diffraction patterns are characteristic of perovskites and show structures that reflect the presence of orthorhombic (or tetragonal) distortions induced by Cu doping. It was confirmed that our data for the undoped samples are compatible with the best results reported by other groups ensuring thus the quality of our sample processing conditions and procedures.

The electrical resistivity $\rho(T,x)$ was measured using the conventional four-probe method. To avoid Joule and Peltier effects, a dc current $I = 1\,\mathrm{mA}$ was injected (as a one second pulse) successively on both sides of the sample. The voltage drop V across the sample was measured with high accuracy by a KT256 nanovoltmeter. Fig.1 presents the temperature behavior of the resistivity $\rho(T,x)$ for six $La_{0.7}Ca_{0.3}Mn_{1-x}Cu_xO_3$ samples, with $0 \leq x \leq 0.05$. Notice a rather broad bell-like form of resistivity for the undoped sample (Fig.1a) reaching a maximum at the so-called metal-insulator transition (peak) temperature $T_0(0) = 200\,\mathrm{K}$. Upon Cu doping, two markedly different processes occur. First of all, the Cu-free (left) resistivity peak increases and becomes more narrow (with $T_0(x)$ shifting towards lower temperatures). Secondly, at a higher temperature another (satellite) peak emerges splitting from the original one. It remains virtually unchanged for small x (up to $x_c \simeq 0.03$) and starts to increase for $x > x_c$ until it finally merges with the main (left) peak at the highest doping level of $x = 0.05$.

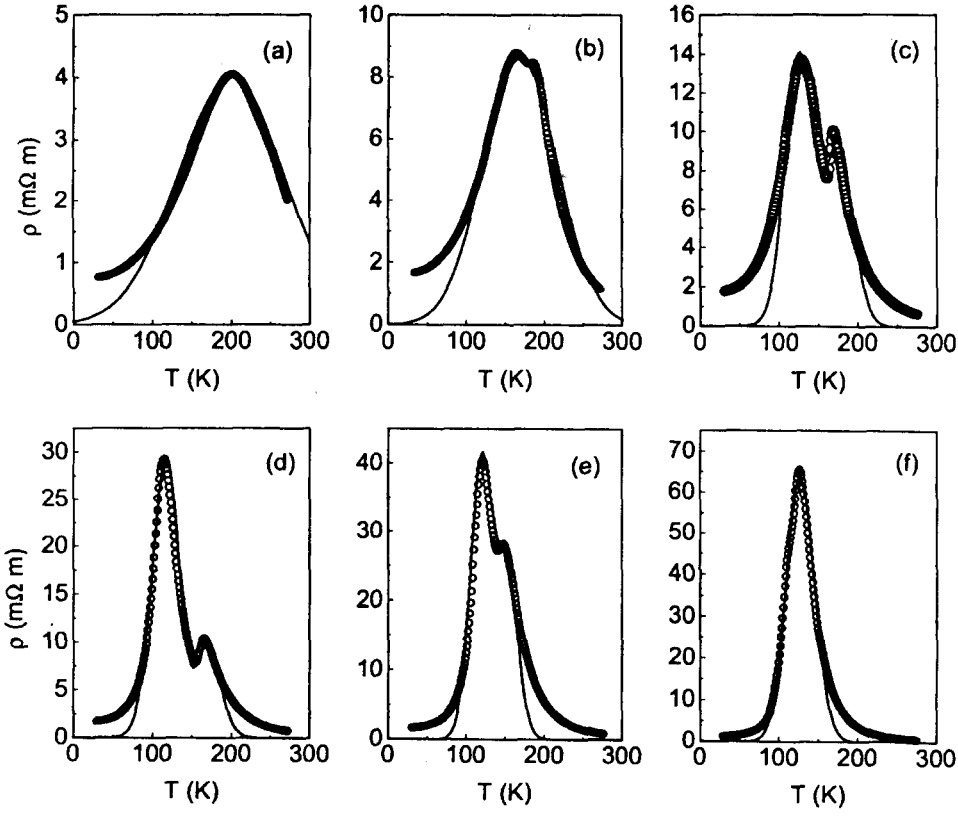

Fig.1.Temperature behavior of the observed resistivity $\rho(T,x)$ in $La_{0.7}Ca_{0.3}Mn_{1-x}Cu_xO_3$ for different copper content: (a) $x = 0$, (b) $x = 0.01$, (c) $x = 0.02$, (d) $x = 0.03$, (e) $x = 0.04$, and (f) $x = 0.05$. The solid lines are the best fits according to Eqs.(3) - (10)

Due to tangible microstructural changes (observed upon copper doping), the JT mechanism plays a decisive role in the above-described resistivity anomalies by assisting electron localization near the M-I transition temperature. Given the growing experimental evidence [14, 15] that polaronic distortions (evident in the paramagnetic state) persist in the ferromagnetic phase as well, we consider the observed resistivity to arise from tunneling of small spin polarons through the doping created potential barriers. According to a conventional picture [5 – 7, 14, 17], the conductivity due to tunneling of a carrier through an effective barrier of height U_{eff} and width R reads

$$\sigma = \sigma_h e^{-2R/L}, \tag{1}$$

where $L = h/\sqrt{2mU_{eff}}$ is a characteristic length with h the Plank's constant and m an effective carrier mass.

To account for the observed anomalous behavior of the resistivity in our samples, we assume that around the metal-insulator transition in addition to the Cu-doping induced slight modification ($x \ll 1$) of the barrier's height $U(x) \equiv U_{eff}(T_0, x) \simeq xU_1 + (1-x)U_2$, the effective potential $U_{eff} = U(x) - E(T,x)$ will also depend on the temperature via the corresponding dependence of the carrier's energy $E(T,x) = h^2/2m\xi^2(T,x)$ with some characteristic length $\xi(T,x) \simeq \xi_0(x)/[1-T/T_0(x)]$ (with [17] $\xi_0(x) \simeq \xi_0(0)/(1-x)^2$) which

plays a role of the charge carrier localization length above T_0 (in insulating phase) and the correlation length below T_0 (in metallic phase), so that $\xi^{-1}(T_0, x) = 0$. Furthermore, given a rather wide temperature dependence of resistivity for the undoped sample (see Fig.1a), we adopt the effective medium approximation scheme and assume a random distribution of hopping distances R with the normalized function $f(R)$ leading to

$$\rho \equiv < \sigma^{-1} > = \frac{1}{Z} \int_0^{R_m} dR f(R) \sigma^{-1}(R), \tag{2}$$

for the effective medium resistivity, where $Z = \int_0^{R_m} dR f(R)$ with R_m being the largest hopping distance. In what follows, for simplicity we consider a Gaussian distribution (around a mean value R_0) with the normalized function $f(R) = (2\pi R_0^2)^{-1/2} e^{-R^2/2R_0^2}$ resulting in the following expression for the observed resistivity

$$\rho(T, x) = \rho_h e^{\gamma^2} \left[\frac{\Phi(\gamma) - \Phi(\gamma - \gamma_m)}{\Phi(\gamma_m)} \right], \tag{3}$$

where

$$\gamma(T, x) = \sqrt{\mu(x) - \gamma_0(x) \left[1 - \frac{T}{T_0(x)} \right]^2}, \tag{4}$$

with

$$\mu(x) = \frac{2mU(x)R_0^2}{h^2} \equiv \mu(0) + x\Delta\mu, \tag{5}$$

(which measures the substitution induced potential barriers $U(x)$ hampering the charge hopping between neighboring Mn sites) and

$$\gamma_0(x) = R_0^2/\xi_0^2(x) \simeq \gamma_0(0)(1 - x)^4 \tag{6}$$

(which measures the effects due to the carrier's kinetic energy $E_0(x) \equiv E(0, x)$, see above). Here $\rho_h = 1/\sigma_h$, $\gamma_m = R_m/R_0$, and $\Phi(\gamma)$ is the error function.

Turning to the discussion of the main (left) resistivity profile, we note that the Cu induced changes of its peak temperature $T_0(x)$ are well fitted by the exponential law

$$T_0(x) = T_0(0) - T_m \left(1 - e^{-x\tau}\right), \tag{7}$$

with $T_0(0) \doteq 200\,\mathrm{K}$, $T_m = 73\,\mathrm{K}$ and $\tau = 56$. At the same time, according to Eqs.(3)-(7) (and in agreement with the observations, see Fig.2), the corresponding peak resistivity $\rho_0(x) \equiv \rho(T_0, x)$ increases with x as follows

$$\rho_0(x) = \rho_0(0) e^{x\Delta\mu}, \tag{8}$$

yielding $\rho_0(0) = \rho_h e^{\mu(0)} = 4\,\mathrm{m\Omega m}$, and $\Delta\mu = 54$ for the model parameters and suggesting that $\rho_0(x) \propto 1/T_0(x)$. To further emphasize this similarity, Fig.2 depicts the extracted doping variation of the normalized quantities, $[T_0(0) - T_0(x)]/T_m$ (open dots) and left peak conductivity $\sigma_0(x)/\sigma_0(0) = \rho_0(0)/\rho_0(x)$ (solid dots) along with the fitting curves (solid lines) according to Eqs.(7) and (8).

A more careful analysis of Eq.(3) shows that in addition to the main peak at $T_0(x)$, equation $d\rho(T, x)/dT = 0$ has two more conjugated extreme points at $T = T_S^{\pm}(x)$ intrinsically linked to the main peak, viz.

$$T_S^-(x) = T_0(x) \left[1 - \sqrt{\frac{\mu(x) - \mu^-}{\gamma_0(x)}} \right] \quad \text{and} \quad T_S^+(x) = T_0(x) \left[1 - \sqrt{\frac{\mu^+ - \mu(x)}{\gamma_0(x)}} \right]$$

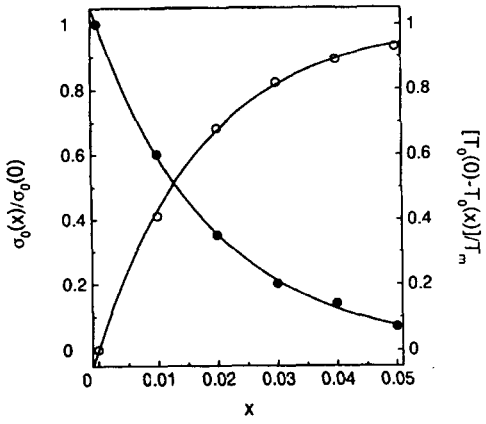

Fig.2. The dependence of the normalized left peak temperature $[T_0(0) - T_0(x)]/T_m$ (open dots) and conductivity $\sigma_0(x)/\sigma_0(0)$ (solid dots) on copper doping x in $La_{0.7}Ca_{0.3}Mn_{1-x}Cu_xO_3$. The solid lines are the best fits according to Eqs.(7) and (8)

with $\mu^{\pm} = \sqrt{2}(2 \pm \gamma_m)$. To attribute these temperatures to the observed satellite (right) peak (see Fig.1), first of all, we have to satisfy the "boundary conditions" at zero ($x = 0$) and highest ($x = x_m = 0.05$) doping levels by assuming $T_S^-(0) = T_0(0)$ and $T_S^+(x_m) = T_0(x_m)$ which lead to the following constraints on the model parameters: $\mu^- = \mu(0)$ and $\mu^+ = \mu(x_m)$. And secondly, to correctly describe the observed evolution of the satellite peak with copper doping and to introduce a critical concentration parameter x_c into our model, we use the continuity condition $T_S^+(x_c) = T_S^-(x_c)$. As a result, we find that the satellite's peak is governed by the unique law over the whole doping interval with

$$T_S^-(x) = T_0(x)\left[1 - \sqrt{\frac{x}{2x_c}}\right], \qquad 0 \le x < x_c, \tag{9}$$

$$T_S^+(x) = T_0(x)\left[1 - \sqrt{1 - \frac{x}{2x_c}}\right], \qquad x_c \le x \le x_m, \tag{10}$$

where $x_m = 2x_c$ with $x_c = \gamma_0(0)/\Delta\mu$. Noting that according to Eqs.(4)-(10), $\gamma^2(T_S^-) = \mu(0)$ and $\gamma^2(T_S^+) = \mu(0) + 2(x - x_c)\Delta\mu$, in good agreement with the observations (see Fig.1) it follows now from Eq.(3) that indeed the satellite peak shows practically no changes with x (up to $x \simeq x_c$) since $\rho_S^-(x) = \rho_h \exp[\gamma^2(T_S^-)] \simeq \rho_0(0)$ and starts to increase above the threshold (for $x > x_c$) as $\rho_S^+(x) = \rho_0(0)\exp[2(x - x_c)\Delta\mu]$ until it totally merges with the main peak at $x \simeq x_m$. By comparing the above expressions with our experimental data for resistivity peaks at $x = x_c$ and $x = x_m$, we get $\gamma_0(0) = R_0^2/\xi_0^2(0) \simeq 1.5$ which (along with extracted above value of $\Delta\mu$, see Eq.(8)) leads to $x_c = \gamma_0(0)/\Delta\mu = E_0(0)/\Delta U \simeq 0.03$ for the critical concentration of copper, in very good agreement with the observations. As expected, x_c reflects the competition between the carrier's kinetic energy and the copper induced potential barrier. In turn, assuming as usual [5, 6, 14, 17] $R_0 \simeq 5.5$ Å for a mean value of the hopping distance and using a free-electron mass value for m, the above estimates yield $U_2 \equiv U(0) \simeq E_0(0) \simeq 0.1$ eV and $U_1 \simeq \Delta U \simeq 3$ eV for the barrier's height of the undoped and maximally doped samples, respectively.

Finally, given the above explicit dependencies for $T_0(x)$ and $T_S^{\pm}(x)$ along with the fixed model parameters, we are able to fit *all* the resistivity data with a single function $\rho(T, x)$ given by Eq.(3). The solid lines in Fig.1 are the best fits according to this equation assuming nearest-neighbor hopping approximation (with $\gamma_m = 1$).

In summary, due to the competition between the copper modified kinetic carrier's energy $E(0,x)$ and the potential barriers $U(x)$ between $Mn^{3+} - Mn^{4+}$ dominated hopping sites, a rather unusual "double-peak" behavior of the resistivity $\rho(T,x)$ is observed in $La_{0.7}Ca_{0.3}Mn_{1-x}Cu_xO_3$ at slight Cu doping around the metal-insulator transition temperature $T_0(x)$. The temperature and x dependencies of the resistivity are rather well fitted by a coherent (nonthermal) tunneling of charge carriers with heuristic expressions for the effective potential $U_{eff}(T,x) = U(x) - E(T,x)$ and the critical concentration of copper x_c.

Part of this work has been financially supported by the Action de Recherche Concertées (ARC) 94-99/174. S.S. thanks FNRS (Brussels) for some financial support.

---

1. H.Y.Hwang, S-W.Cheong, P.G.Radaelli et al., Phys. Rev. Lett. **75**, 914 (1995).
2. J.Fontcuberta, M.Martinez, A.Seffar et al., Phys. Rev. Lett. **76**, 1122 (1996).
3. T.T.M.Palstra, A.P.Ramirez, S-W.Cheong et al., Phys. Rev. **B56**, 5104 (1997).
4. J.Fontcuberta, V.Laukhin, and X.Obradors, Appl. Phys. Lett. **72**, 2607 (1998).
5. M.Viret, L.Ranno, and J.M.D.Coey, Phys. Rev. **B55**, 8067 (1997).
6. L.Sheng, D.Y.Xing, D.N.Sheng et al., Phys. Rev. Lett. **79**, 1710 (1997).
7. L.P.Gor'kov and V.Z.Kresin, JETP Lett. **67**, 985 (1998).
8. N.A.Babushkina, L.M.Belova, O.Yu.Gorbenko et al., Nature (London) **391**, 159 (1998).
9. N.A.Babushkina, L.M.Belova, V.I.Ozhogin et al., J. Appl. Phys. **83**, 7369 (1998).
10. A.M.Balagurov, V.Yu.Pomyakushin, V.L.Aksenov et al., JETP Lett. **67**, 705 (1998).
11. N.A.Babushkina, L.M.Belova, D.I.Khomskii et al., Phys. Rev. **B59**, 6994 (1999).
12. A.M.Balagurov, V.Yu.Pomyakushin, D.V.Sheptyakov et al., JETP Lett. **69**, 50 (1999).
13. A.M.Balagurov, V.Yu.Pomjakushin, D.V.Sheptyakov et al., Phys. Rev. **B60**, 383 (1999).
14. S.Sergeenkov, H.Bougrine, M.Ausloos et al., JETP Lett. **70**, 141 (1999).
15. M.Rubinstein, D.J.Gillespie, J.E.Snyder et al., Phys. Rev. **B56**, 5412 (1997).
16. K.Ghosh, S.B.Ogale, R.Ramesh et al., Phys. Rev. **B59**, 533 (1999).
17. S.Sergeenkov, H.Bougrine, M.Ausloos et al., JETP Lett. **69**, 858 (1999).